Heliyon 9 (2023) e12742

Contents lists available at ScienceDirect

Heliyon

journal homepage: www.cell.com/heliyon

Research article

An algorithm for cognitive fusion targeted tumor puncture based on 3-D mathematical modelling

Yong Luo [a,1], Junjie Ren [b,1], Jun Long [c], Li Wang [d,***], Hong Zeng [e,**], Dali Tong [a,*]

[a] Department of Urology, Daping Hospital, Army Medical University, Chongqing, 400042, China
[b] School of Sciences, Southwest Petroleum University, Chengdu, 610500, Sichuan, China
[c] Department of Ultrasound, Chongqing Health Center for Women and Children, Chongqing, 401147, China
[d] Department of Gastrointestinal Surgery, Daping Hospital, Army Medical University, Chongqing, 400042, China
[e] Department of Urology, Traditional Medicine Hospital of Jiangjin District, Chongqing, 402260, China

ARTICLE INFO

Keywords:
Precise percutaneous tumor puncture
Radiological data
Space analytic geometry
Mathematical modelling
Algorithm

ABSTRACT

Background: Percutaneous puncture is an important means of tumor diagnosis and treatment. At present, most puncture operations are still based on imaging location and clinical experience, and quantitative and accurate targeted puncture cannot be achieved. How to improve the accuracy of percutaneous tumor puncture, avoid errors to the greatest extent, reduce the occurrence of complications, and improve the overall clinical diagnosis and treatment quality and curative effect, are scientific problems worthy of further study.

Method: In the present study, mathematical modeling was first used to construct the tumor puncture path, determine the needle entry angle, and define the relevant limited parameters and the substitution formula. Secondly, relevant parameters were extracted from CT and other imaging data and substituted into formulas, the deviation angle and puncture path were determined, and the personalized tumor puncture scheme was carried out. Third, targeted puncture was precisely implemented under the guidance of B-ultrasound. Compared with the traditional empirical puncture, our model improved the accuracy, decreased the puncture time, and reduced the pain of diagnosis and treatment for patients.

Results: A tumor-targeted puncture model was established based on mathematical theory and imaging data. By extracting clinical data, such as tumor radius, projection distance of tumor center and projection distance from puncture point to body surface, the optimal puncture deviation angle was modeled and calculated and a personalized puncture scheme was established. Compared with the conventional method, our model markedly increased the puncture accuracy rate by ~30%. The puncture number was decreased by ~50% using our model. Furthermore, our model shortened the operation time by 20% to ease pain of patients and guarantee greater security for patients. Doctor satisfaction and patient discomfort scores were examined. Our model improved doctor satisfaction by ~20% and reduced subjective discomfort of patients by ~25%. These data revealed that the model could markedly improve the accuracy and efficiency of puncture, clinical efficacy and accuracy of tumor diagnosis. Additionally, the confidence of doctors in the operation was greatly enhanced and patient discomfort was greatly reduced.

* Corresponding author.
** Corresponding author.
*** Corresponding author.
E-mail addresses: wanglitmmu@163.com (L. Wang), zyyzh123@163.com (H. Zeng), tongdali1985@163.com (D. Tong).
[1] These authors have contributed equally to this work.

https://doi.org/10.1016/j.heliyon.2022.e12742
Received 14 January 2022; Received in revised form 26 December 2022; Accepted 26 December 2022
Available online 30 December 2022

Conclusion: The present study analyzed in detail how to find the best puncture path using a mathematical model. Based on the mathematical model of cognitive fusion puncture, combined with clinical personalized data and mathematical calculation analysis, accurate puncture was effectively realized. It not only greatly improved the effectiveness of puncture, but also ensured the safety of clinical patients and reduced injury, which means it may be worthy of clinical application.

1. Introduction

Image-guided percutaneous biopsy is the cornerstone of histological diagnosis of tumors. Furthermore, the ability to safely sample tissue in locations that previously required surgery or necessitated empiric therapy has allowed for more personalized treatment options. Percutaneous tumor puncture allows clinicians to quickly extract tumor samples from patients, identify pathological types, detect tissue genes and analyze molecular biology, and enables local targeted therapy. Therefore, mastering the percutaneous tumor puncture technique and reasonably planning the puncture path can greatly improve the clinical efficacy.

Percutaneous tumor puncture generally requires imaging assistance, including brightness modulation (B-mode) ultrasound and an X-ray machine such as computed tomography and C-arm X-ray. There are several requirements for radiological equipment: 1. Help define the location of the tumor and examine the local prolife; 2. Assure the relationship with the tumors or anatomical markers around; 3. Find the optimum puncture target and escape important tissue such as vessels; 4. Most importantly, select the optimum puncture route [1,2].

Percutaneous tumor biopsies have achieved good accuracy in diagnosing cancer based on clinical trials, systematic review and meta-analysis of multiple organs. In a systematic review and meta-analysis of the diagnostic accuracy of percutaneous renal tumor biopsy (RTB) in 57 studies including 5228 patients, the overall median diagnostic rate of RTB was 92%. The sensitivity and specificity of diagnostic percutaneous core biopsy or fine-needle aspiration were 99.1% and 99.7%, and 93.2% and 89.8%, respectively. RTB has good accuracy in diagnosing renal cancer and its subtypes, and it appears to be safe [3]. However, there are reports about misdiagnosis, technical failure cases and secondary puncture of percutaneous tumor biopsy. A study of quantitative pre-operative pancreatic biopsy data reported that the mean accuracy of diagnosis was 95.76% (range, 91–100). Furthermore, the procedure had a high negative

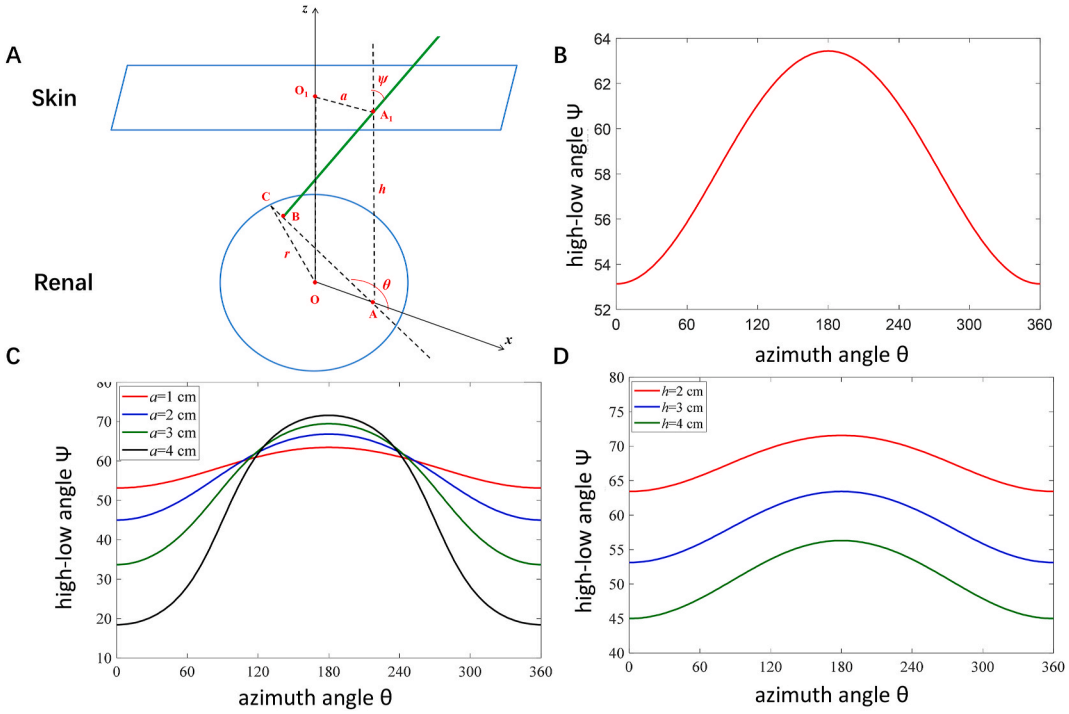

Fig. 1. A. Schematic of puncture route based on the mathematical model. The projection of point A1 on the kidney plane is A, the direction of the OA line is defined as the x-axis, the direction of the oo1 line is defined as the z-axis, and the angle between the needle and the positive direction of the z-axis is ψ (i.e., elevation angle). Suppose that the insertion point of the needle in the kidney is B, and the angle between the line AB and the positive direction of the x-axis is θ (that is, azimuth). B. Value of the upper limit of the elevation angle ψ_{max} for different azimuth angles θ; C. Relationship between azimuth θ and the upper limit of high and low angles ψ_{max} for different deviation distances a; D. Relationship between azimuth θ and the upper limit of high and low angles ψ_{max} for different skin-kidney distances h.

predictive value of ~76.26%. Of the 13 reported studies, 7.3% were inadequate or technical failure cases. The mean rate of complications was 2.08% [4]. Therefore, how to improve the accuracy of percutaneous tumor puncture, avoid errors to the greatest extent, reduce the occurrence of complications, and improve the overall clinical diagnosis and treatment quality and curative effect are scientific problems worthy of further study.

Traditional percutaneous tumor puncture requires the help of B-mode ultrasound or X-ray. Our current model is based on both mathematical calculations and B mode-guided cognitive fusion targeted tumor biopsy. In the present study, we presented the tumor as the model of cognitive fusion puncture. The concept mainly builds on 3D-model construction and mathematical calculation and focuses on noninvasive and precise puncture. Compared with conventional puncture, the technique markedly increased successful rates of pinpoint attack, decreased puncture times and iatrogenic injury, and better controlled operation and post-operation complications. The approach on cognitive fusion tumor-targeted puncture was proposed based on radiological data, space analytic geometry and mathematical modelling [5,6].

2. Mathematical model

In order to standardize precise puncture well, a mathematical model was used to explain the puncture route and angle range.

2.1. Model description

As shown in Fig. 1A, there are skin and kidney in the vertical direction. Suppose that the horizontal section of the kidney is a circle with the radius being r. The center of the kidney is denoted by O, and the projection of the O on the skin plane is O1. The distance between the skin and the kidney is $|O_1O| = h$. If a needle is used to pierce from the skin to the kidney, the insertion point (A1) of the needle on the skin deviates from the O1 with the distance $|O_1A_1| = a$. How to adjust the angle of the needle so that the needle can finally reach the kidney.

2.2. Model establishment

The coordinate system was established, and the needle insertion angle was defined. As shown in Fig. 1A, assuming that the projection of point A1 on the kidney plane is A, the direction of the OA line is defined as the x-axis, the direction of the OO1 line is defined as the z-axis, and the angle between the needle and the positive direction of the z-axis is ψ (i.e., elevation angle). Suppose that the insertion point of the needle on the kidney is B, and the angle between the line AB and the positive direction of the x-axis is θ (that is, azimuth angle).

Suppose that the azimuth angle θ is determined first when inserting the needle, ask what the range of the elevation angle ψ should be in order to ensure that the needle can reach the kidney.

As shown in Fig. 1A, line AB intersects the circle at point C. We know that $|OC| = r$, $|OA| = a$, $\angle OAC = \pi - \theta$。 Supposing $a \le r$ and according to the cosine theorem for ΔOAC, we can obtain that:

$$|OC|^2 = |AC|^2 + |OA|^2 - 2|AC| \cdot |OA| \cdot \cos(\pi - \theta) \tag{1}$$

Substituting $|OC| = r$ and $|OA| = a$ into equation (1), we get:

$$r^2 = |AC|^2 + a^2 - 2|AC| \cdot a \cdot \cos(\pi - \theta) \tag{2}$$

By solving equation (2), we can get the following results calculated based on equation (3):

$$|AC| = -a \cdot \cos\theta + \sqrt{a^2 \cdot \cos^2\theta - a^2 + r^2} \tag{3}$$

The distance $|AB|$ can be obtained by the following equation (4):

$$|AB| = |AA_1| \cdot \tan\psi = h \cdot \tan\psi \tag{4}$$

To ensure that the needle can reach the kidney, $|AB| \le |AC|$ should be satisfied, that is:

$$h \cdot \tan\psi \le -a \cdot \cos\theta + \sqrt{a^2 \cdot \cos^2\theta - a^2 + r^2} \tag{5}$$

Considering $0 \le \psi \le \frac{\pi}{2}$ and equation (5), we can get the value range of ψ when the needle can reach the kidney:

$$0 \le \psi \le \arctan\frac{-a \cdot \cos\theta + \sqrt{a^2 \cdot \cos^2\theta - a^2 + r^2}}{h} \tag{6}$$

2.3. Model validation

Several points need to be defined before the operation: 1. The indication confirmation for nephrostomy; 2. CT-scan used for evaluating primary anatomical structure and seeking suitable puncture locations; 3. Building a pre-constructed structure chart for mathematical calculation; 4. Combination of CT data and the puncture azimuth to ascertain a, r, θ and h, and substitution of these data into equation (6) to obtain the range of ψ; 5. After defining the range, performing cognitive fusion tumor-targeted puncture with the

help of ultrasound.

Example 1. When $|O_1A_1| = a = 0$, what should the range of the elevation angles ψ be to ensure that the needle could reach the kidney

Analysis: When $|O_1A_1| = a = 0$, the insertion point of the needle on the skin is just located above the center O of the kidney. According to equation (6), it can be obtained that no matter what the azimuth value θ, $0 \le \psi \le \arctan\frac{r}{h}$ should be satisfied.

Example 2. Supposing $r = 5$ cm, $a = 1$ cm, $h = 3$ cm, the value range of elevation angles ψ for different azimuth angles θ can be obtained. According to equation (6), it is known that the lower limit of ψ is always equal to 0. In fact, we are concerned about the upper limit of ψ, which is expressed as:

$$\psi_{\max} = \arctan\frac{-a\cdot\cos\theta + \sqrt{a^2\cdot\cos^2\theta - a^2 + r^2}}{h}$$

Fig. 1B shows the value of the upper limit of the elevation angle $\psi_{\max}$ under different azimuth angles θ. When the azimuth angle is $\theta = 180°$, the value range of the elevation angle ψ to ensure that the needle can reach the kidney is the largest (i.e., $0° \le \psi \le 63.4°$); when the azimuth angle is $\theta = 0°$ or $\theta = 360°$, the value range of the elevation angle ψ to ensure that the needle can reach the kidney is the smallest (i.e., $0° \le \psi \le 53.1°$).

In the following, the sensitive analysis of parameters a and h on the $\psi_{\max}$ is carried out. Fig. 1C shows the relationship between the azimuth angle θ and the upper limit of the elevation angle $\psi_{\max}$ for different deviation distances a. It can be seen that the larger the deviation distance a is, the larger the variation range of the upper limit of the elevation angle $\psi_{\max}$ is.

Fig. 1D shows the relationship between the azimuth angle θ and the upper limit of the elevation angle $\psi_{\max}$ for different skin-kidney distances h. It can be seen that the change trend between the azimuth angle θ and the upper limit of the elevation angle $\psi_{\max}$ is the same for different skin-kidney distances h. As h increases, the upper limit of the elevation angle $\psi_{\max}$ decreases.

3. Clinical data, validation and analysis of model accuracy

In the present study, mathematical modeling was first used to construct the tumor puncture path, determine the needle entry angle, and define the relevant limited parameters and the substitution formula. Secondly, relevant parameters were extracted from CT and other imaging data, substituted into formulas, the deviation angle and puncture path were determined, and the personalized tumor puncture scheme was generated. Third, targeted puncture was precisely implemented under the guidance of B-ultrasound. Compared with traditional empirical puncture, our model improved the accuracy, decreased the puncture time and reduced the pain of diagnosis and treatment for patients.

3.1. Extraction of clinical data

Extraction of clinical data was based on the CT scan. A 64-slice spiral CT was used to check potential tumors. Conventional plain and contrast-enhanced CT scanning were performed to localize tumors according to the manufacturer's instructions. The tumor data were positioned, qualitatively determined and further identified by professional physician and experienced clinician combined with

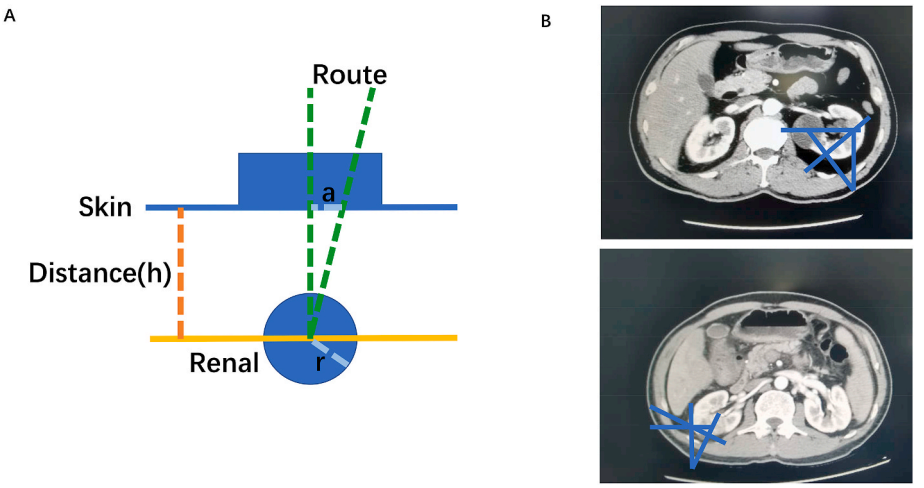

Fig. 2. Schematic model of puncture route (A) and CT-guided puncture route (B). Based on the previous proposed model, the schematic model of the puncture route was designed. The parameters r, a and h are required to obtain $\psi_{\max}$. In the CT image, the values of three parameters were calculated by defining the puncture point and route. r represents the tumor radius; a represents the distance between the puncture point and body surface projection of the tumor center; h represents the distance between the body surface projection and tumor center.

multidisciplinary cooperation [7].

The puncture path, which met certain conditions, including avoiding organs and barriers, and having a low puncture difficulty, was first designed based on CT imaging. Based on our model, data, including the values of r, a and h, were extracted from the CT image analysis. The θ value was further calculated based on the puncture azimuth. Fig. 2A and B indicate how to define the puncture angle and path based on model calculation and imaging.

3.2. Mathematical calculation

According to r, a, h and θ, the $\psi_{\max}$ value can be obtained via the calculation formula:

$$\psi_{\max} = \arctan \frac{-a \cdot \cos\theta + \sqrt{a^2 \cdot \cos^2\theta - a^2 + r^2}}{h}$$

In other words, puncture within this angle is sure to succeed. An angle larger than this angle will lead to puncture of the area outside the tumor. If we locate the skin puncture point and choose different puncture azimuths s to puncture or fine tune, we will get different θ values. Thus, different $\psi_{\max}$ values will be obtained based on the aforementioned formula. Therefore, accurate puncture path design and puncture angle calculation will greatly improve the success rate of puncture and minimize errors.

3.3. B-mode ultrasound-guided puncture

Ultrasound measurements can be made using B-mode. B-mode scans produce a two-dimensional image of the underlying tissue. Routine scans are done at 3.5–5 Mhz in abdominal examination (The model has also been considered for use in percutaneous puncture of multiple organs, including the thyroid gland and mammary gland, and in patients with weak muscle. Therefore, the choice of high or low frequency B-ultrasound should be determined according to the actual situation). A convex probe is usually used for visualization in the abdomen. A linear probe should be mainly used in the chest, thyroid and blood vessels. The B-mode uses high-resolution images to determine the subcutaneous depth [8]. Therefore, knowledge of the technical piece based on computational model construction will not only largely improve operation ability and accuracy but also benefit patients.

According to the aforementioned methods and calculated values, tumor puncture was performed under the guidance of B-ultrasound. A total of 19 cases were punctured based on our model with accurate calculation, while 19 cases were punctured with conventional methods based on clinical experience alone. The values of various parameters are listed in SupplementalTable through calculation based on our model. The study was approved by the Research Ethics Committee of Daping Hospital, Army Medical Center, Army Medical University and Traditional Medicine Hospital of Jiangjin district. Informed consent was obtained from all patients/participants for your experiments. The images were provided by the Department of Medical Imaging.

The radius of the tumor and the distance from the skin were determined based on images. These data can be substituted into the formula for mathematical calculation. A rough range of two types of angles, Ψ and θ, can be obtained. According to the angles, we combined with intraoperative ultrasound localization to design an appropriate puncture path. When determining the puncture angle and route during the operation, the assistant usually assists the chief surgeon to determine the puncture route using an angle measurer. At present, 19 operations have been completed based on our model with 19 negative control cases as a general model. The clinical outcomes of our model have been demonstrated based on our assessment of model accuracy and patient benefits. The mathematical model is explained in the methods section and the clinical experience is reported in the results section as previously described. We

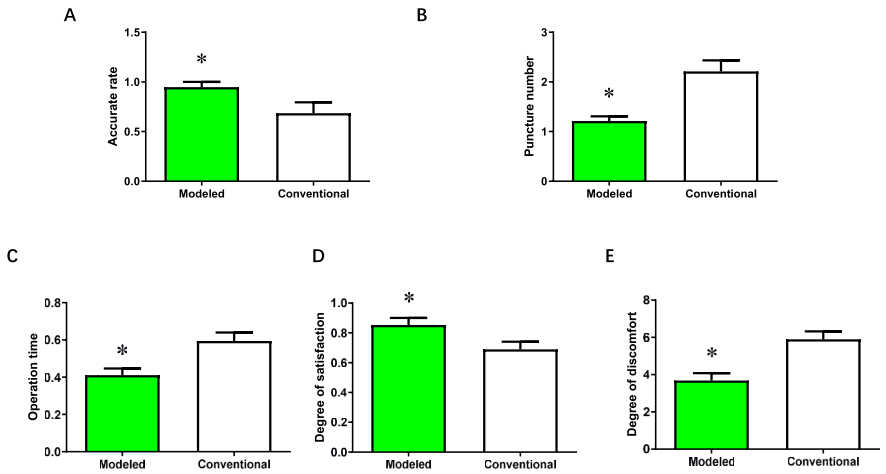

Fig. 3. Accuracy rate (A), puncture number (B), operation time (C), degree of satisfaction (D) and the degree of discomfort (E) were compared between the conventional method group and the proposed model group. Comparisons between two groups were conducted using unpaired Student's t-test. A value of $P < 0.05$ was considered to be statistically significant. * indicates $P < 0.05$.

agree that it is important to know how the angles were executed. In the model, the best deviation angle Ψ was obtained based on mathematical modeling, parameter extraction and formula calculation. During the operation, the angle and puncture path were selected with the help of an angle gauge and some fixtures.

4. Results

Several indexes were used to evaluate the clinical efficacy and benefits: Puncture accuracy rate, puncture number, operation time, uncomfortable symptoms scores and satisfaction degree of doctors. Compared with the conventional method, our model markedly increased the puncture accuracy rate by ~30% (Fig. 3A). These data are mainly based on cross reference with postoperative histopathological diagnosis. Furthermore, the puncture number was decreased by ~50% using our model (Fig. 3B). These data indicated that the model could improve the accuracy and efficiency of puncture. These improve clinical efficacy and accuracy of tumor diagnosis. Furthermore, our model shortened the operation time by 20% to ease pain of patients and guarantee greater security for patients (Fig. 3C). In order to further demonstrate the superiority of our model, doctor satisfaction and patient discomfort scores were examined. Based on the acquired results, our model improved doctor satisfaction by ~20% (Fig. 3D)and reduced the subjective discomfort of patients by ~25% (Fig. 3E). These subjective scoring data indicated that the puncture path based on model construction and data calculus was more accurate and confident, which greatly increased the uncertainty of relying solely on clinical experience. Additionally, based on the accurate puncture path, the number of puncture needles with low error and the doctors' determination to operate, the discomfort of patients and the inevitable damage caused by iatrogenic diagnosis and treatment could be greatly reduced (Fig. 3).

Fig. 4 shows a schematic diagram of our workflow including the clinical application of the mathematical model and the assessment of clinical outcome. In the present study, the mathematical model was first proposed, then the required data were extracted from images and mathematical calculation was performed, and finally clinical data, validation and analysis of the model accuracy were provided.

5. Discussion

Percutaneous tumor puncture is applied in both clinical diagnosis and treatment. It has the advantages of easy operation, less trauma and rapid diagnosis. At the same time, it has clear indications for tumors with insufficient clinical evidence, unclear imaging examination and alternative treatment options. Therefore, it has always been the first-line standard of tumor diagnosis and treatment. However, in operations in clinical settings, the problems of unsuccessful puncture and false positive and false negative errors are

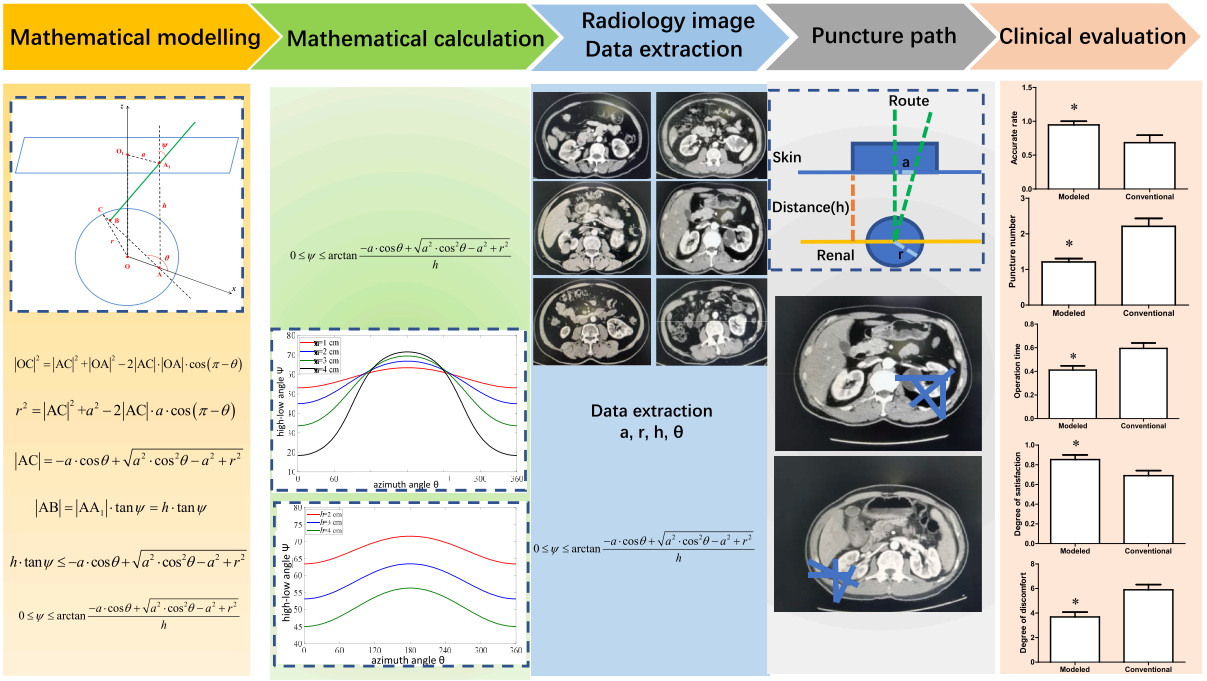

Fig. 4. Schematic of our proposed model. A puncture model was first constructed based on trigonometric function and analytic geometry, then the calculation formula of the best puncture angle and the necessary indicators were clarified to obtain the best angle, the best puncture angle was calculated based on the image extraction data, and then targeted precise tumor puncture was performed according to the puncture angle. Finally, the clinical application potential of the model was evaluated according to the puncture efficiency, clinical benefit and subjective score.

encountered. Therefore, the implementation of standardized, individualized and accurate percutaneous tumor puncture can minimize the error rate, failure rate and repeated puncture rate, minimize the pain of patients and obtain accurate pathological evidence, which has great clinical benefits [9,10]. In the present study, it was analyzed in detail how to find the best puncture path using a mathematical model. Based on the mathematical model of cognitive fusion puncture combined with clinical personalized data and mathematical calculation analysis, the accurate puncture was effectively realized. It not only greatly improved the effectiveness of puncture, but also ensured the safety of clinical patients and reduced injury, which suggests that it is worthy of clinical application [11].

A targeted tumor puncture model was constructed through space analytic geometry and trigonometric function, and then personalized imaging data were extracted and substituted into the model to determine the three-dimensional puncture path. The key point is to determine the value range of the two core angles in the puncture path. Different angle combinations were selected to complete the operation of percutaneous tumor puncture with the cooperation of assistants [12,13]. In the verification in clinical cases, our model was more accurate than traditional puncture, with fewer complications and better clinical benefits. In fact, certain types of tumors in exogenesis and endogenesis are also applicable in the method because of accuracy. The technique is used to obtain pathological evidence to distinguish original and metastatic tumors, as well as benign and malignant tumors. With the help of ultrasound, the puncture range can be defined and easily escape blood vessels supplying tumor growth.

How to accurately analyze the objective data calculated from the model and minimize the error in practical operation is the key to accurate puncture. The number of puncture cases, learning curve, clinical experience of the chief surgeon and the accurate cooperation of assistants are all key factors for the success of puncture. Therefore, the integration of mathematical modeling and cognition is required for smooth operation. The presentation of cognitive fusion tumor-targeted puncture.

The perspective of cognitive fusion tumor-targeted puncture was proposed based on radiological data, space analytic geometry and mathematical modelling. The puncture route uses cartesian coordinates (polar coordinates) or valid transformation of coordinates in the description of geometric shapes. Cognitive fusion puncture helps urologists diagnose various diseases, including prostate cancer and other types of cancer, based on cognitive fusion MRI-guided prostate puncture and CT-guided tumor puncture. Furthermore, cognitive fusion tumor-targeted puncture for nephrostomy achieves maximal accuracy and minimal injury, and may potentially be applied in urological obstruction. Previously, cognitive fusion puncture has been successfully applied in urological systems, including MRI-guided prostate cancer puncture. The presentation of the tumor as the model of cognitive fusion puncture is novel. The concept mainly builds on 3D-model construction and mathematical calculation and focuses on noninvasive and precise puncture. Compared with conventional puncture, the technique markedly increased successful rates of pinpoint attack, decreased puncture times and iatrogenic injury, and better controlled operation and post-operation complications. At present, cognitive fusion targeted tumor puncture is still in the preliminary stage of combining clinical experience with imaging. The model system we proposed is based on actual data extracted from imaging and combined with actual clinical work experience to design a personalized puncture path. This work effectively improves the participation of cognitive fusion in targeted puncture and makes the puncture path design more scientific, accurate and efficient. However, there is still a long way to go to fully integrate cognitive fusion and other artificial intelligence fields into clinical operations.

The model design proposed is the modeling of three-dimensional space. Modeling-based simulation biology design and medical equipment development are potential directions in the future. The current application of ultrasound-guided equipment is not enough to achieve accurate puncture. The two-dimensional puncture without modeling guidance has certain errors in theory and has the limitations of clinical experience [14]. Thus, doctors without clinical puncture experience require a long learning curve. Therefore, the design of simulated puncture medical equipment based on imaging can accurately assist puncture and greatly reduce the threshold of clinical operation [15]. Our design idea is based on imaging evaluation and calculation, data extraction and mathematical modeling,

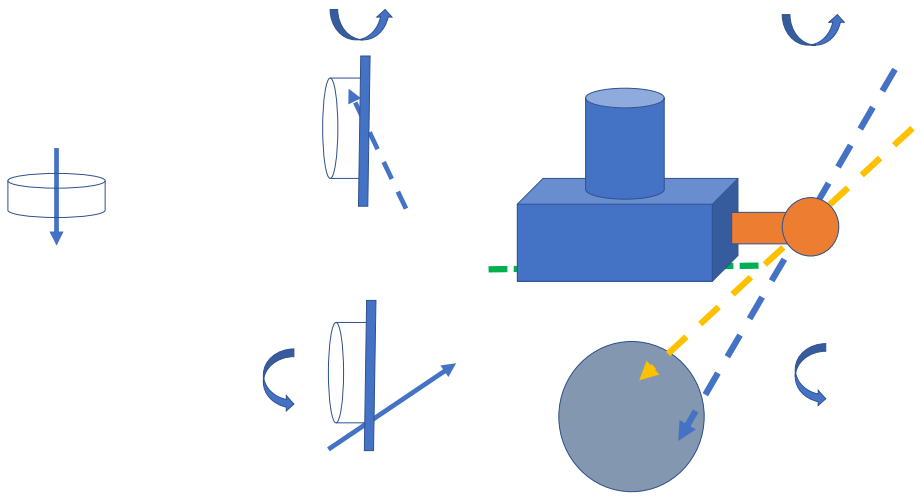

Fig. 5. Concept map of a connecting rod ultrasonic equipment that can adjust the puncture angle. Based on the proposed puncture model and the clinical benefit verification, a concept map of a connecting rod ultrasonic equipment that can adjust the puncture angle was generated.

and puncture parameters (angle and distance, etc.) are determined and combined with simulated biological equipment for accurate puncture. This requires interdisciplinary cooperation and collaborative research by clinicians, mathematicians and bioengineers (Fig. 5). Based on the proposed puncture model and the clinical benefit verification, a concept map of a connecting rod ultrasonic equipment that can adjust the puncture angle was generated.

Declarations

Authors' contributions

Dr. Dali Tong, Dr. Yong Luo and Dr. Junjie Ren conceived, designed and performed the experiments. Dr. Li Wang, Dr. Hong Zeng and Dr. Dali Tong analyzed and interpreted the data. Dr. Jun Long conducted ultrasound help. Dr. Hong Zeng and Dr. Dali Tong contributed partial materials and data support. Dr. Yong Luo, Dr. Junjie Ren and Dr. Dali Tong wrote the paper

Funding

This work was in part supported by Dr. Dali Tong Chongqing Science and Technology Bureau (Basic and Frontier Research Project; grant no. cstc2018jcyjAX0645), Dr. Dali Tong Chongqing Municipal Health and Health Committee (Science and Health Joint Medical Research Project; grant no. 2018QNXM041) and Dr. Dali Nursery Talents Fund of Army Medical University.

Availability of data and materials

The datasets used and/or analyzed during the current study are available from the corresponding author on reasonable request.

Ethics approval and consent to participate

The study was approved by the Research Ethics Committee of Daping Hospital, Army Medical Center, Army Medical University and Traditional Medicine Hospital of Jiangjin district. Written informed consent from the patient were obtained the for the use of related images. The images were provided by the Department of Medical Imaging.

Consent for publication

The authors agree with the publication.

Declaration of competing interest

The authors declare that they have no known competing financial interests or personal relationships that could have appeared to influence the work reported in this paper.

Appendix A. Supplementary data

Supplementary data related to this article can be found at https://doi.org/10.1016/j.heliyon.2022.e12742.

References

[1] W.A. Berg, Image-guided breast biopsy and management of high-risk lesions, Radiol. Clin. 42 (2004) 935–946, vii.
[2] W. Hong, E.J. Hwang, J.H. Lee, J. Park, J.M. Goo, C.M. Park, Deep learning for detecting pneumothorax on chest radiographs after needle biopsy: clinical implementation, Radiology 303 (2022) 433–441.
[3] L. Marconi, S. Dabestani, T.B. Lam, F. Hofmann, F. Stewart, J. Norrie, A. Bex, K. Bensalah, S.E. Canfield, M. Hora, et al., Systematic review and meta-analysis of diagnostic accuracy of percutaneous renal tumour biopsy, Eur. Urol. 69 (2016) 660–673.
[4] Y. Huang, J. Shi, Y.Y. Chen, K. Li, Ultrasound-guided percutaneous core needle biopsy for the diagnosis of pancreatic disease, Ultrasound Med. Biol. 44 (2018) 1145–1154.
[5] M. Akand, A. Buyukaslan, S. Servi, L. Civcik, A hypothetical method for calculation of the access point, direction angle and access angle for percutaneous nephrolithotomy, Med. Hypotheses 124 (2019) 101–104.
[6] H. Hongzhang, Q. Xiaojuan, Z. Shengwei, X. Feixiang, X. Yujie, X. Haibing, K. Gallina, J. Wen, Z. Fuqing, Z. Xiaoping, et al., Usefulness of real-time three-dimensional ultrasonography in percutaneous nephrostomy: an animal study, BJU Int. 122 (2018) 639–643.
[7] H.Y. Qin, H. Sun, X. Wang, R. Bai, Y. Li, J. Zhao, Correlation between CT perfusion parameters and microvessel density and vascular endothelial growth factor in adrenal tumors, PLoS One 8 (2013), e79911.
[8] D.R. Wagner, B.J. Thompson, D.A. Anderson, S. Schwartz, A-mode and B-mode ultrasound measurement of fat thickness: a cadaver validation study, Eur. J. Clin. Nutr. 73 (2019) 518–523.
[9] L. Li, X.L. Xu, K. Feng, X.Q. Liu, J. Yang, Benign pathologies results from lung nodule percutaneous biopsies: how to differentiate true and false benign? J. Cancer Res. Therapeut. 17 (2021) 658–663.
[10] R.E. Overman, T.T. Kartal, A.J. Cunningham, E.A. Fialkowski, B.J. Naik-Mathuria, S.A. Vasudevan, M.M. Malek, R. Kalsi, H.D. Le, L.C. Stafford, et al., Optimization of percutaneous biopsy for diagnosis and pretreatment risk assessment of neuroblastoma, Pediatr. Blood Cancer 67 (2020), e28153.

[11] K. Saba, M.S. Wettstein, L. Lieger, A.M. Hotker, O.F. Donati, H. Moch, D.P. Ankerst, C. Poyet, T. Sulser, D. Eberli, et al., External validation and comparison of prostate cancer risk calculators incorporating multiparametric magnetic resonance imaging for prediction of clinically significant prostate cancer, J. Urol. 203 (2020) 719–726.
[12] X. Lin, L. Ma, K. Du, J. Hong, S. Luo, Y. Lai, Y. Dai, X. Kong, Application of a treatment planning system-assisted large-aperture computed tomography simulator to percutaneous biopsy: initial experience of a radiation therapist, J. Int. Med. Res. 49 (2021), 300060520983141.
[13] H. Zhang, Y. Guang, W. He, L. Cheng, T. Yu, Y. Tang, H. Song, X. Liu, Y. Zhang, Ultrasound-guided percutaneous needle biopsy skill for peripheral lung lesions and complications prevention, J. Thorac. Dis. 12 (2020) 3697–3705.
[14] A. van der Aa, C.K. Mannaerts, M.C.W. Gayet, J.C. van der Linden, B.P. Schrier, J.P.M. Sedelaar, M. Mischi, H.P. Beerlage, H. Wijkstra, Three-dimensional greyscale transrectal ultrasound-guidance and biopsy core preembedding for detection of prostate cancer: Dutch clinical cohort study, BMC Urol. 19 (2019) 23.
[15] J. Yang, J. Zhu, D.Y. Sze, L. Cui, X. Li, Y. Bai, D. Ai, J. Fan, H. Song, F. Duan, Feasibility of augmented reality-guided transjugular intrahepatic portosystemic shunt, J. Vasc. Intervent. Radiol. 31 (2020) 2098–2103.